Natural Working Fluids for Absorption Refrigeration

Marianne Kerleaux, Laurence Rodier, Jean-Michel Andanson, Alain Dequidt, Yohann Coulier

DOI 10.18462/iir.gl2022.xxx

Natural Working Fluids for Absorption Refrigeration

Marianne Kerleaux[(a)], Laurence Rodier[(a)], Jean-Michel Andanson[(a)], Alain Dequidt[(a)], Yohann COULIER*[(a)]

[(a)] Université Clermont Auvergne, CNRS, SIGMA Clermont, Institut de Chimie de Clermont-Ferrand
F-63000 Clermont-Ferrand, France
*Corresponding author: yohann.coulier@uca.fr

ABSTRACT

European and global regulations on greenhouse gases are constantly evolving. Most of the fluorinated refrigerants currently used are close to be banned due to their high global warming potentials. Therefore new alternatives less harmful to the environment need to be developed. Our goal is to identify new natural refrigerant/absorbent pairs for an absorption refrigeration process. To limit the environmental impact of the working fluid pairs used, the natural refrigerant will be carbon dioxide and the absorbent will be a compound derived from biomass. This work presents the developed methodology to select potential biobased solvent to be used with CO2 in an absorption refrigeration process.

Keywords: Refrigeration, Carbon Dioxide, Biobased solvent, absorption.

1. INTRODUCTION

To mitigate greenhouse gas emissions and prevent further environmental degradation, the refrigerant alternatives have become a hot topic in the refrigeration industry. Indeed the search for alternatives to vapor-compression refrigeration has become more critical since refrigeration and air-conditioning industries have to find refrigerants with zero Ozone-Depleting Potential (ODP) and Global Warming Potential (GWP) lower than 150 (Mota-Babiloni et al., 2017). An alternative to this process is absorption refrigeration which presents several advantages such as a low work input requirement and the chance to use natural refrigerant/absorbent pairs(Srikhirin et al., 2001). Typical commercially available absorption systems use combinations of water/lithium bromide (LiBr) for moderate temperature applications, and ammonia/water for low temperature. Nevertheless, these working fluids exhibit specific issues such as technological challenges, or health hazards, or environmental concerns which prevent wider use. To overcome some of these problems, the use of ionic liquids (ILs) as absorbents to replace water in ammonia/water system or LiBr has been investigated (Kim et al., 2012, Wasserscheid Seiler, 2011).

Many different fluid combinations have been tried so far, and new ones are constantly being sought (Macriss et al., 1988, Sun et al., 2012). Performance of an absorption cycle is critically dependent on the thermodynamic properties of working fluids (Perez-Blanco, 1984). Main required properties of refrigerant/absorbent pairs are:

- low volatility of the absorbent;
- high solubility of the refrigerant in the absorbent;
- low heat of mixing of refrigerant and absorbent;
- favorable heat and mass transfer;
- no crystallization or solidification.

Both refrigerant and absorbent should be non-corrosive, environmental friendly, and low-cost.

In this work, new biobased combinations of refrigerant and absorbent were identified. The challenge of fluid combinations search was made simpler by selecting the refrigerant beforehand. The proposed refrigerant is carbon dioxide (CO_2 or R744). It is one of the few natural refrigerants, which is neither flammable nor toxic. It is inexpensive, widely available and have a very low impact on the global

environment (GWP=1) (Lorentzen, 1994). Furthermore, CO_2 offers significant advantages in cooling applications such as high thermal conductivity and latent heat. The absorbent will be an organic compound derived from the biomass. Thus the vapor absorption refrigeration process will use a bio-based solvent in which the carbon dioxide gas will be absorbed.

The components of a classical vapor absorption refrigeration cycle are an absorber, a generator, a condenser, an expansion valve and an evaporator. Here, the high temperature conditions and high operating pressure, will yield to use a CO_2 transcritical cycle. The condenser is thus replaced by a gas cooler. Only the carbon dioxide will circulate to the evaporator and heat exchangers. The vapor leaving the evaporator will be absorbed into the bio-based solvent in the absorber. The pressure of the mixture of refrigerant and absorbent will then be increased with a liquid pump. The generator would heat this mixture to vent the refrigerant. The remaining liquid, will flow back through an expansion valve to the absorber. The high pressure high temperature CO_2 leaving the generator will be cooled transferring thus heat to the surrounding environment. Then the pressure of the refrigerant will be reduced by passing through an expansion valve in order to be converted to vapor in the evaporator, thus extracting heat to the enclosed space to be cooled.

This study proposes an original methodology based on the combination of three complementary scientific fields covering the areas of knowledge required for the design of working pairs for absorption refrigeration namely:

- the development of simulation tools to help in the selection of potential bio-based absorbent,
- the acquisition of key thermodynamic data to assess the potential candidate pairs,
- the development of thermodynamic models to simulate the process.

First this work introduces the methodology developed to select potential bio-based absorbents to be used with CO_2. From this approach more than twenty BBSs were identified. Five of them are presented in this paper namely ethyl levulinate (E-LEV), γ-butyrolactone (GBL), dibutyl succinate (DBS), cyrene (CYR) and anisole (ANI). As mentioned before, one of the fundamental requirements for absorption refrigeration process is the high refrigerant absorption capacity. For all these BBSs except cyrene, experimental vapor-liquid equilibrium (VLE) data are available from literature (Deng et al., 2015, Giacomin Junior et al., 2019, Kim et al., 1989, Li et al., 2016, Park et al., 1991, Xu et al., 2003). New experimental VLE data for {CO_2+cyrene} system were determined in this work using a calorimetric technique and a spectroscopic technique. All these experimental data were used to validate the force field of the molecular simulations (the way atoms interact) and select an appropriate thermodynamic model capable of reproducing phase equilibria. Finally, this thermodynamic model was used to compare CO_2 solubility in the five BBS at the operating conditions of the absorber and the regenerator.

2. MATERIALS AND METHODS

2.1. Absorbent selection methodology

Recent studies have shown that the ability of organic solvents to absorb CO_2 is closely related to their molecular structure (Gwinner et al., 2006). Comparisons of CO_2 solubility in various absorbents have shown that carbonyl, ether, and ester groups in a solvent enhance CO_2 absorption (Gui et al., 2014). A review of the literature of BBSs based on molecular structures with carbonyl, ether or ester group(s) was carried out to obtain a preselection of approximately 100 potential solvents. An approach using molecular descriptors led then to the selection of the best matching solvents for basic requirements of a vapor absorption refrigeration cycle. For example, since apolar solvents have a low CO_2 transport capacity and small solvent molecules are highly volatile, simple descriptors such as the ratio of oxygen per carbon atom or molecular weight have been used. Finally, a reduced list of about 20 solvents was obtained by excluding compounds with properties incompatible with the process, such as melting temperature above 253 K; boiling temperature below 423 K; viscosity greater than 10 cP at 298 K and flash point below 298K. Five BBSs from this list are listed together with their key thermophysical properties in Table 1.

Table 1. Physical properties of solvents used in the present study

Name	Structural formula	MW /g·mol^{-1}	Melting point /K	Boiling point /K	Viscosity /cP	Flash point /K
E-LEV	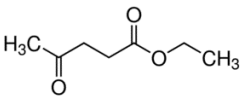	144.17	201.0	478.6	1.93[a]	364
GBL		86.09	229.6	477.2	1.75[a]	371.5
DBS	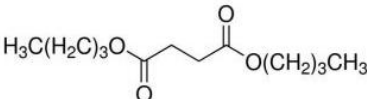	230.30	244.2	548.5	3.52[a]	417
CYR	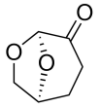	128.13	255.0	499.9	1.67[a]	381
ANI	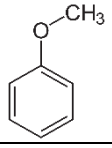	108.14	235.6	426.9	1.52[b]	325

[a] at 298K and [b] at 288K

A key condition of an efficient combination between refrigerant + absorbent is that the absorbent should have a strong affinity for the refrigerant at the condition of temperature and pressure of the absorber. Experimental vapour liquid equilibrium data of {CO_2 +BBS} systems are available for EL, GBL, DBS and ANI (Table 2) but not for CYR. To compare CO_2 solubility in these solvents, molecular simulations were investigated. In the same time a thermodynamic model using an equation state was developed. For that purpose, new experimental VLE data were determined for {CO_2 +CYR} system.

Table 2: Literature data for the solubility of CO2 in the 4 selected bio-based solvents

Compounds	*T* / K	*p* / MPa	Reference
EL	283.15 – 323.15	0 – 0.6	Deng et al., 2015
	303.15 – 353.15	2 – 14	Giacomin Junior et al., 2019
GBL	285 – 373	2.5 – 70	Li et al., 2016
	313 – 363	9 – 27	Xu et al., 2003
DBS	283.15 – 323.15	0 – 0.6	Deng et al., 2015
Anisole	333.2 – 393.2	4.1 – 18.3	Park et al., 1991
	343.1 – 372.3	2.4 – 16.8	Kim et al., 1989

2.2. **Computational procedures**

The simulations were performed using the LAMMPS simulation software (Thompson et al., 2022) following an automated process. The CO_2 was modeled using the EPM2 force field while the solvent was modeled with the OPLS force field (Jorgensen Tirado-Rives, 2005) using parameters from the ligpargen online tool (Dodda et al., 2017). The cross interactions between CO_2 and the solvent were determined using geometric mixing rules. The long range interactions beyond the cutoff of 10 Å were computed using the PPPM method

with a precision of 10^{-4}. This includes Coulomb interactions and the $1/r^6$ part of the Lennard-Jones interactions.

The number of molecules and the initial box size were determined by fixing the target composition, the total mass around 136×103 amu and the density at 1 $g.cm^{-3}$. The molecules were put into the simulation box using the packmol tool (Martínez et al., 2009).

The simulations consisted of 3 stages. In the first stage, the system was compacted to a dense phase by applying a high pressure of 1000 bar for 5 ns. Then the box size was extended in the z direction by a factor 3 by inserting vacuum. In the second stage, the system was equilibrated at constant volume for 10 ns. The goal was to let the liquid vapor equilibrium take place. The final stage was identical to the second stage, but data were collected and averaged: density profiles and normal pressure P_{zz}. During the 3 stages, the temperature was fixed to its target value using a Langevin thermostat with a characteristic time of 3 ps. The time step was 1 fs and bonds involving H atoms were constrained using the shake algorithm. All the simulations were performed at 283 and 323.5 K. Only the results at the highest temperature are given in this work because the equilibration at the lowest temperature was not always reached during the simulation process.

Finally, from the density profiles, the compositions of the liquid and vapor phases were computed. The liquid vapor phase diagram at constant temperature was drawn by plotting P_{zz} as a function of the liquid and vapor compositions. In practice, since the chosen solvents were not volatile, the vapor contains only CO_2 molecules.

2.3. **Experimental studies**

Experimental studies were conducted to determine the solubility of CO_2 in cyrene at 313.15 K and pressures from 0.5 to 4 MPa. For that purpose, an original approach combining a flow calorimetric and a spectroscopic technique was developed. The calorimetric technique allowed to determine with accuracy the solubility of CO_2 in cyrene at 4.00 MPa. Nevertheless, this technique requires large amounts of solvent. Therefore, IR spectroscopy was used as a complementary technique to quickly measure numerous data point but with a lower precision.

2.3.1. Materials

Cyrene™ BioRenewable (dihydrolevoglucosenone) was purchased from Merck with a purity of > 99 % and was used without further purification. Carbon dioxide (purity of 99.995 %) was obtained from Air Products.

2.3.2. Calorimetric study

The experimental technique used in this work to measure the enthalpy of solution of CO_2 in the absorbent has already been described in detail by Arcis et al. (Arcis et al., 2011) The enthalpy of solution ($\Delta_{sol}H$) of CO_2 in cyrene is determined as a function of gas loading α (mol CO_2/mol cyrene), using a flow-mixing cell custom-made for a BT2.15 calorimeter from Setaram. Experiments were performed at constant temperature (±0.03 K) and pressure (±0.005 MPa). The absorbent solution and the carbon dioxide were mixed into the mixing cell located in the calorimetric block where the heat flux due to gas dissolution is measured. The two fluids flow at constant volume flow rate using two high-pressure syringe pumps (Isco Model 260 DM). To maintain a constant molar flow rate, the pumps are temperature-controlled at 298.15 ± 0.1 K. The molar flow rates are derived from the volume flow rates of the pumps using fluid densities. The densities of CO_2 were calculated using the equation of state from Span and Wagner (Span Wagner, 1996) and the densities of cyrene are issued from (Baird et al., 2019). The enthalpy of solution $\Delta_{sol}H$ is derived from the calorimetric signal difference, detected by the thermopile surrounding the mixing cell as follows:

$$\Delta_{\mathrm{sol}}H \,/\, \mathrm{kJ}\cdot\mathrm{mol}^{-1} = \frac{(S_{\mathrm{M}} - S_{\mathrm{BL}})}{K\dot{n}_i} \qquad \text{Eq. (1)}$$

where subscript *i* is for CO_2 or cyrene, and *K* is a calibration constant used to convert the calorimetric signal (mV) into heat flux (mW). S_M represents the thermopile signal during the mixing process and S_{BL} the baseline signal recorded only when cyrene is flowing through the calorimeter. The molar enthalpy is calculated using the molar flow rates $\dot{n}_i$ (mol s^{-1}) of the gas ($\Delta_{sol}H$/kJ mol^{-1} of CO_2, Figure 1a) or the molar flow rate of amine ($\Delta_{sol}H$/kJ mol^{-1} of amine, Figure 1b). The relative uncertainties on loading charge and enthalpies of solution are less than 1.5% and 5%, respectively (Arcis et al., 2011).

2.3.3. Spectroscopic study

IR spectra were measured on around 0.5 ml of cyrene in a cylindric cell of about 2ml thermostated at 40°C and under various pressure up to 4.0 MPa. This setup was already described in details in a previous publication (Brugère et al., 2020). The ATR (Attenuated Total Reflection)-IR cell was place in a FT-IR Tensor II spectrometer from Bruker Optics equipped with a DTGS (deuterated triglycine sulfate) detector. Spectra were measured in the range between 4000 and 500 cm^{-1} with a resolution of 4 cm^{-1}. The equilibrium of the concentration of CO_2 in cyrene was validated by checking the stability of the IR spectrum during at least 10 minutes with a constant pressure and temperature while the all liquid phase was under vigorous stirring. Equilibration were always obtained in less than 20 minutes.

2.4. **Thermodynamic Modeling**

In this work the experimental data were described using the Soave–Redlich–Kwong (SRK) equation of state (EOS) (Redlich Kwong, 1949, Soave, 1972):

$$P = \frac{RT}{v-b} - \frac{a\alpha(T)}{v(v+b)} \qquad \text{Eq. (2)}$$

With components parameters a_i and b_i:

$$a_i = 0.42748\frac{R^2T_{c,i}^2}{P_{c,i}} \qquad \text{Eq. (3.a.)}$$

$$b_i = 0.08664\frac{RT_{c,i}}{P_{c,i}} \qquad \text{Eq. (3.b.)}$$

And Soave alpha function:

$$\alpha_i(T) = [1+0.480+1.574\omega_i - 0.176\omega_i^2)(1-\sqrt{T/T_{c,i}})]^2 \qquad \text{Eq. (4)}$$

With ω_i the acentric factor of component *i*. The critical pressures and temperatures and the acentric factors of each component are given in Table 3.

Table 3. Characteristic parameters of pure compounds[(a)]

Name	T_c /K	P_c /MPa	ω
CO_2	304.21	7.383	0.22362
E-LEV	666.1	2.924	0.60709
GBL	731.0	5.130	0.40304
DBS	695.38	1.796	0.92620

CYR	774.35	5.166	0.48651
ANI	645.6	4.250	0.35017

[a] from Simulis Thermodynamics compounds properties database

The mixing rules (Eq. (5) and Eq. (6)) and the binary interaction parameters (Eq. (7)) for CO_2-BBS system were expressed using the conventional Van der Walls definition:

$$a\alpha = \sum_i \sum_j z_i z_j \sqrt{(a\alpha)_i (a\alpha)_j}(1-k_{ij}) \quad \text{Eq. (5)}$$

$$b = \sum_i z_i b_i \quad \text{Eq. (6)}$$

$$k_{ij} = k_{ji} \text{ and } k_{ii} = 0 \quad \text{Eq. (7)}$$

For each mixture CO_2–BBS, the value of the binary interaction parameter k_{ij} was obtained by minimizing the following objective function *F* using Simulis Thermodynamic software:

$$F = \sum \left(\frac{P_{\text{exp}} - P_{cal}}{P_{\text{exp}}} \right)^2 \quad \text{Eq. (8)}$$

The available experimental data from literature used for model parameter estimation are given in Table 2.

3. RESULTS AND DISCUSSION

3.1. Experimental result

3.3.1. Calorimetric study

The enthalpy of solution of CO_2 in cyrene was investigated at 313.15 K and 4.0 MPa Experiments were conducted for different gas loading charge (α) values up to the saturation of the absorbent solution. Large exothermic effects were observed. The enthalpies of solution versus loading charge are illustrated in Figure 1. When the enthalpy of solution $\Delta_{sol}H$ is expressed in kJ.mol^{-1} of CO_2 (Figure 1a), the graph exhibits a plateau for the lowest loading charges ($\alpha \leq 0.4$), and then, the exothermic effect decreases as the loading increases. The value of enthalpy of solution at low loading charge, $\Delta_{sol}H^{av}$= -14.6 kJ mol^{-1}, is the average value obtained on the plateau, for $\alpha \leq 0.4$.

In Figure 1b, experimental enthalpies of solution expressed in kJ mol^{-1} of cyrene are plotted as a function of loading charge. These experimental enthalpies exhibit two different domains. In the first domain ($0 < \alpha \leq 0.5$), $\Delta_{sol}H$ increases linearly with the loading charge. The value of the slope corresponds to $\Delta_{sol}H^{av}$ obtained previously (Figure 1a). The second domain, where the enthalpy of solution stays constant, is characteristic of solution saturation. The intersection between unsaturated (enthalpy increase) and saturated (plateau) domains yields the solubility of the gas. The experimental solubility of CO_2 in cyrene at 313.15 K and 4.00 MPa was then graphically determined and is given in Table 4.

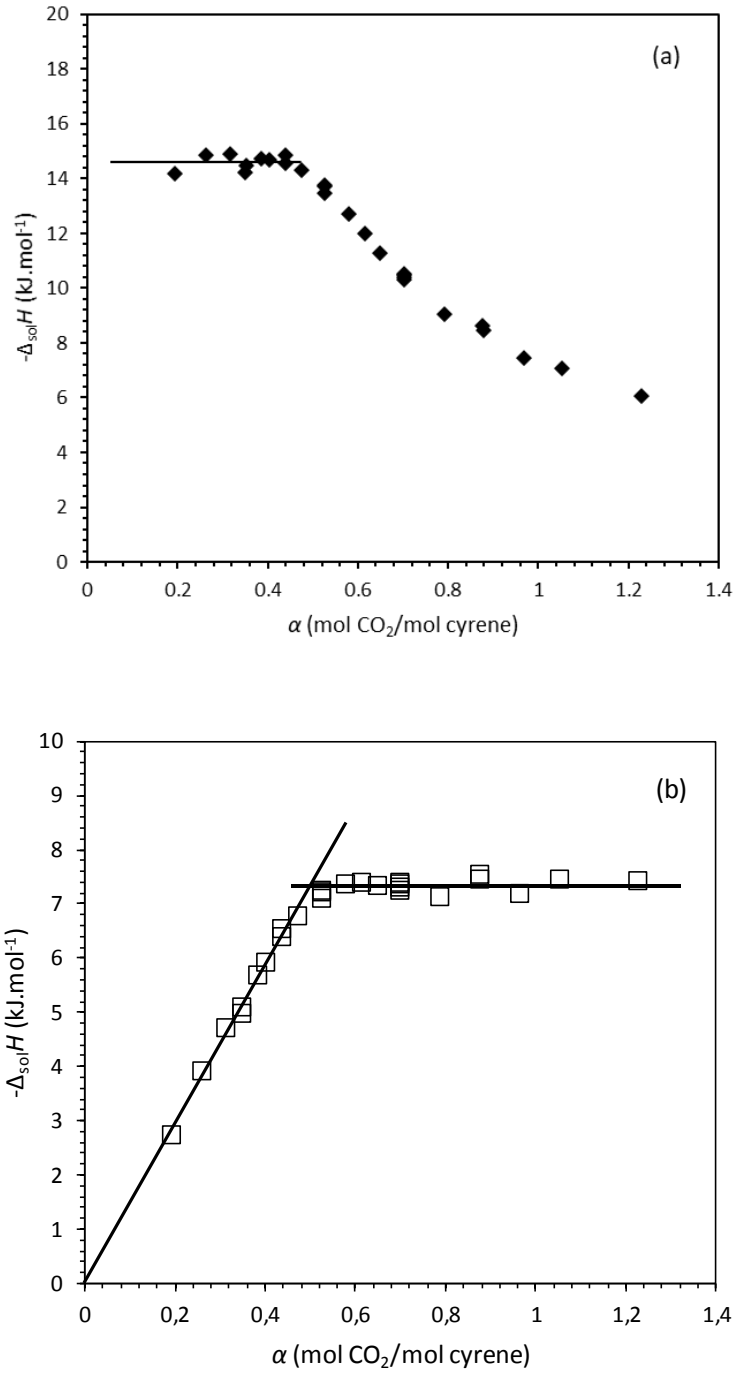

Figure 1. Enthalpy of solution ($-\Delta_{sol}H$) of CO_2 in cyrene versus CO_2 loading (α) at T = 313.15 K and p = 4.00 MPa. (a) $\Delta_{sol}H$/(kJ mol^{-1} of CO_2), straight lines show the average values for the enthalpies of solution at low loadings (α < 0.4). (b) $\Delta_{sol}H$/(kJ mol^{-1} of cyrene).

3.3.2. Spectroscopic study

The evolution of the amount of CO_2 physically absorbed (no chemical reaction between CO_2 and cyrene) in the liquid phase can be estimated by calculating the evolution of the integration of the CO_2 asymmetric stretching band centered around 2340 cm^{-1} or with the bending vibration around 655 cm^{-1} (figure 2). Numerical values of CO_2 solubility in cyrene are reported in Table 4.

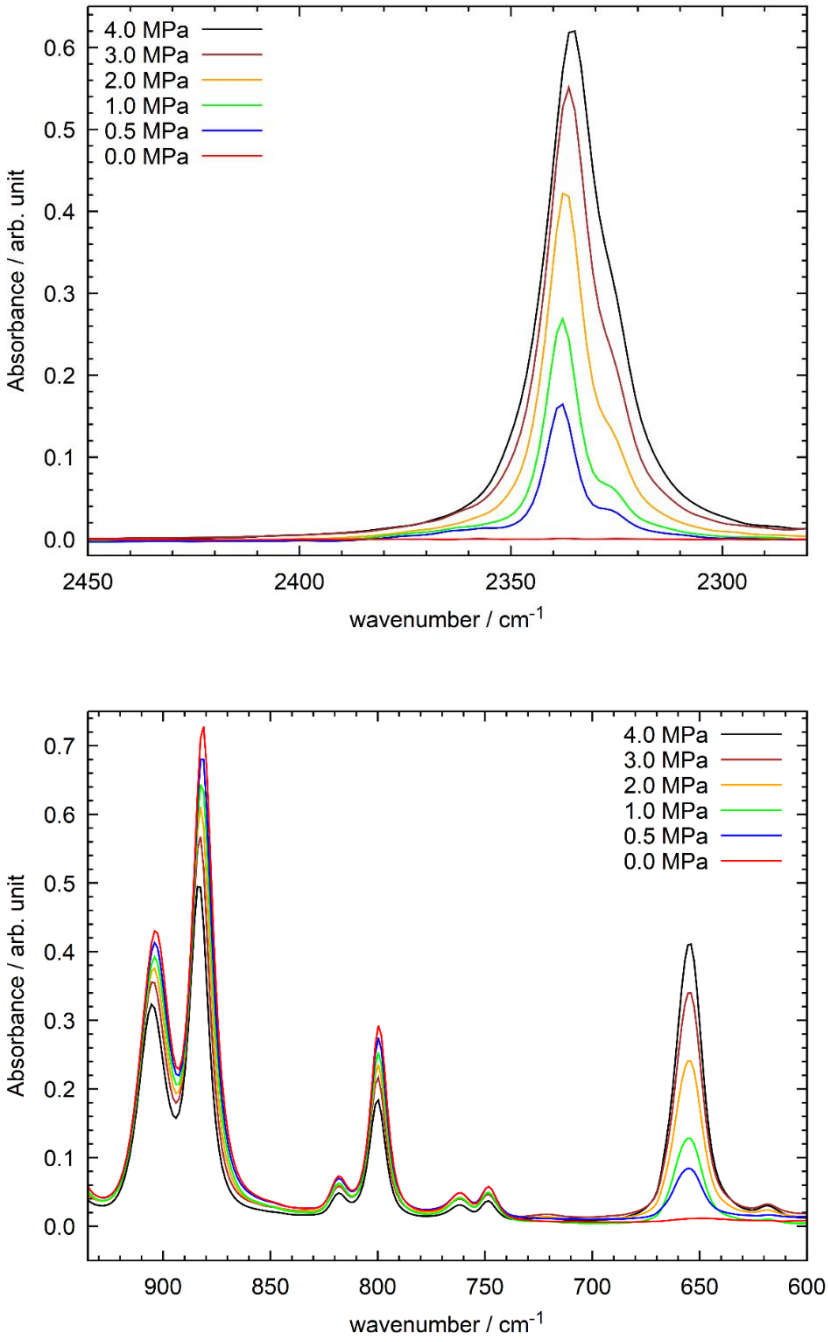

Figure 2: Part of the IR spectra of binary mixture (cyrene + CO_2) at 40°C under pressure up to 4.0 MPa.

Both bands are showing the same increase of the concentration of CO_2 in cyrene while increasing the pressure. On the other hand, bands at 800, 880 or 905 cm^{-1}, corresponding to the signal of the solvent are continuously decreasing with the pressure. All bands of the solvent show the same trend. This decrease corresponds mainly to the swelling of the solvent (Pasquali et al., 2008). Between 0 and 4.0 MPa of CO_2, the swelling can be estimated at around 25%, which indicates that CO_2 have a high solubility in this solvent.

Table 4: Experimental values for the solubility of CO_2 in cyrene at 313.15 K

T^a = 313.15 K					
p^a / MPa	x_{CO2}	$u(x_{CO2})$	p^a / MPa	x_{CO2}	$u(x_{CO2})$

0.50	0.06	0.01	2.50	0.22	0.02
1.00	0.10	0.01	3.00	0.26	0.02
1.50	0.14	0.01	3.50	0.30	0.02
2.00	0.18	0.02	4.00[b]	0.337	0.003

[a] u(T) = 1 K and u(p) = 0.1 MPa - [b] from calorimetric study with u(T) = 0.03 K and $u(p)$=0.005 MPa

3.2. Modeling results

Molecular simulations were performed at 323. 5 K to predict vapor-liquid equilibria of {CO_2+BBS} systems. Predictive values are compared in Figures 3-5 with experimental data for E-LEV, GBL, and DBS for which experimental solubilities are available at this temperature. The estimated values are found to be in agreements with experimental data except for DBS at pressures greater than 3 MPa. From this approach the best candidates for the absorption process are E-LEV, DBS and ANI.

The Soave-Redlich-Kwong equation of state has been used to represent the vapour-liquid equilibria of the five binary systems {CO_2+BBS}. The correlations are illustrated in Figures 3-7. The model allows to correlate the VLE data of the different systems in the whole range of pressure except for DBS where no experimental data are available at high pressure. This model can be used to predict the solubility with a reasonable precision where experimental data are missing.

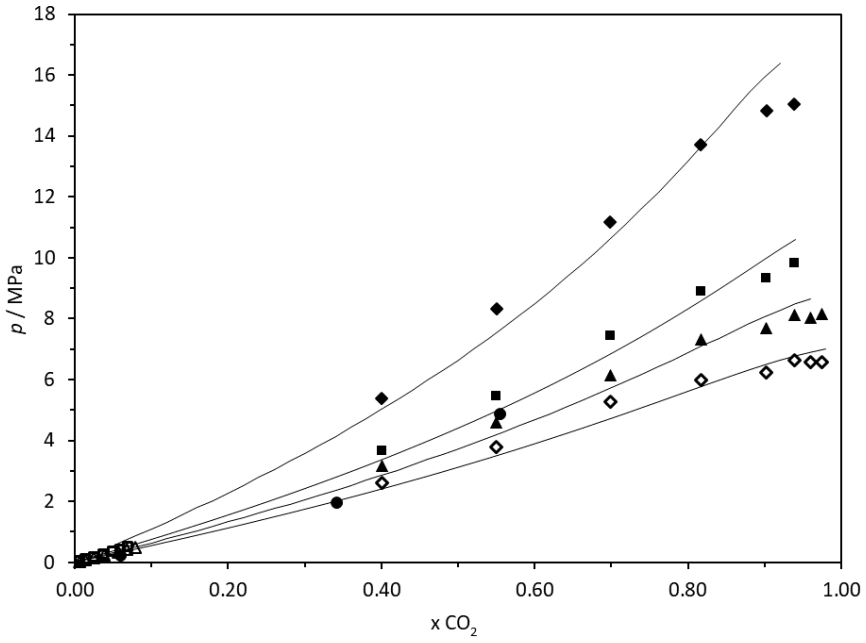

Figure 3. Solubility of CO_2 in ethyl levulinate: ◊ 303.15 K , ▲ 313.5 K, ■ 323.15 K, ♦ 353 K (Giacomin Junior et al., 2019); Δ 313.5 K, □ 323.15 K (Deng et al., 2015); ● molecular simulation at 323.5 K; ── model (k_{ij} = 0.01168).

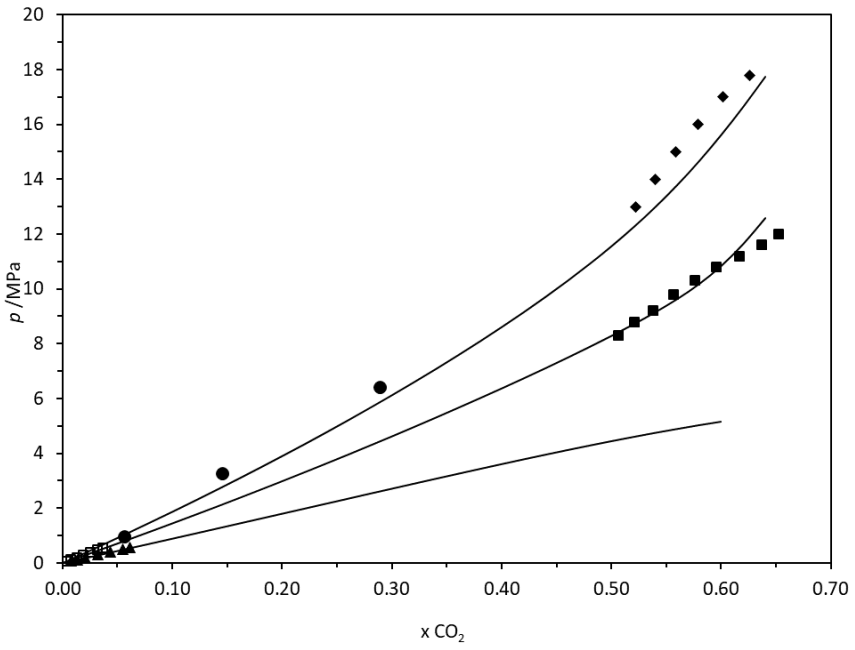

Figure 4. Solubility of CO_2 in γ-Butyrolactone: ▲ 293.15 K, □ 323.15 K (Li et al., 2016); ■ 323.15 K, ♦ 343 K (Xu et al., 2003); ● molecular simulation at 323.5 K; ── SRK (k_{ij} = 0.04399).

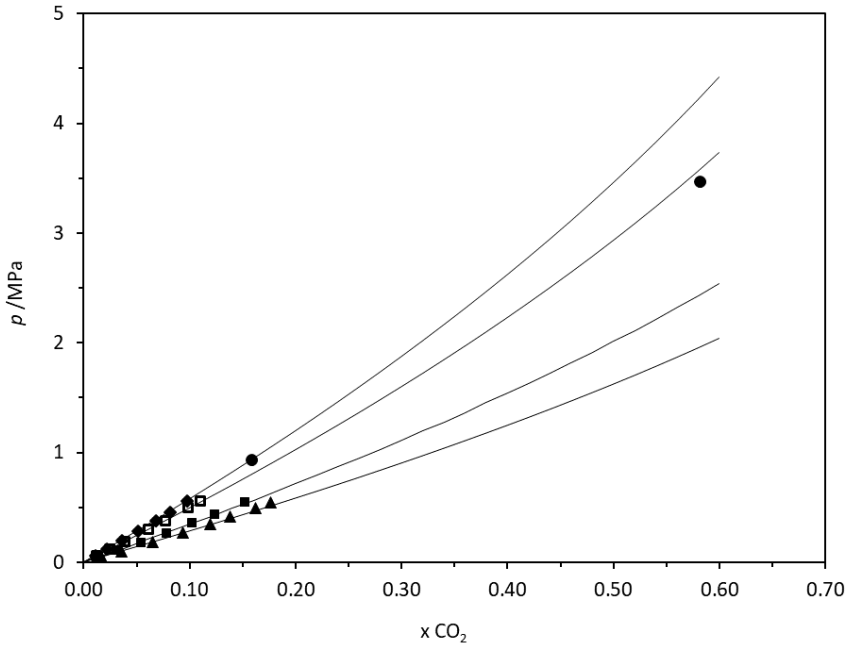

Figure 5. Solubility of CO_2 in dibutyl succinate: ▲ 283.15 K, ■ 293.15 K, □ 313.15 K, ♦ 323.15 K (Deng et al., 2015); ● molecular simulation at 323.5 K; ── SRK (k_{ij} = -0.02855).

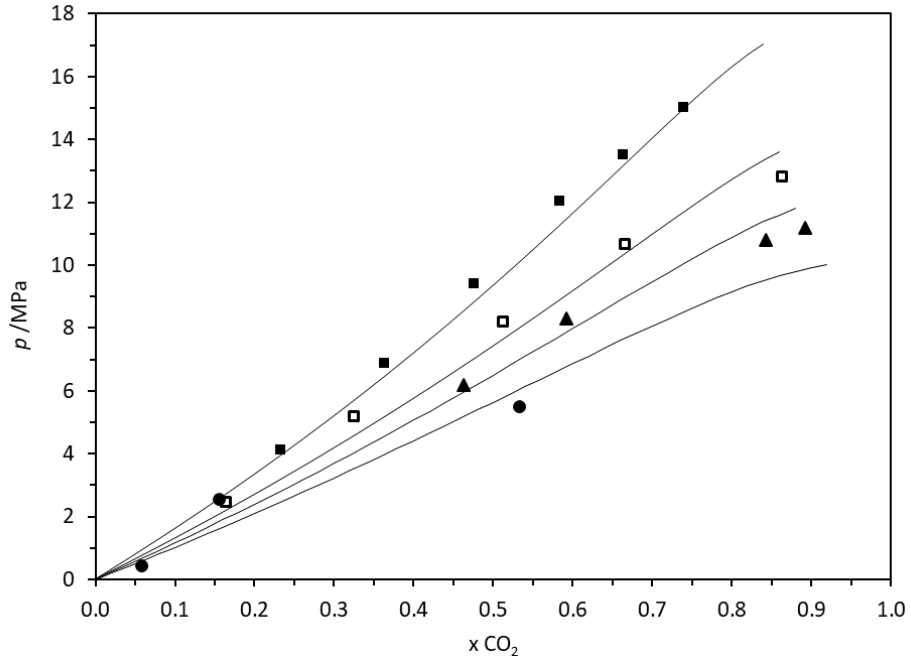

Figure 6. Solubility of CO_2 in anisole: ▲ 333.2 K, ■ 363.3 K (Park et al., 1991); □ 343.1 K (Kim et al., 1989) ; ● molecular simulation at 323.5 K ; ── SRK (k_{ij} = 0.04084).

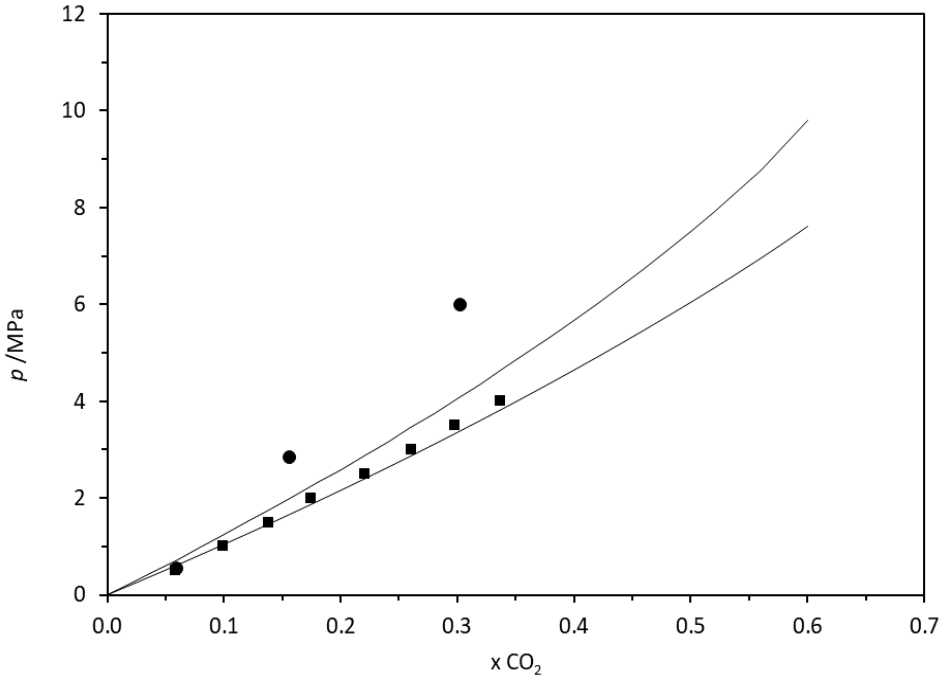

Figure 7. Solubility of CO_2 in cyrene: ■ 313 K (this work); ● molecular simulation at 323.5 K ; ── SRK (k_{ij} = -0.13009).

3.3. Discussion

To assess the potential of these five BBSs, the SRK EOS with the binary parameters adjusted in this work for each system were used to predict CO_2 solubility at 283 K and 353 K. These temperatures were chosen to reproduce the temperature conditions of the absorber and the regenerator of a single-stage vapor absorption cycle. The calculated values are illustrated in Figure 8. At 283 K, DBS, E-LEV and ANI are the absorbents for which CO_2 has the highest affinity. This result agrees with the molecular simulation

predictions established in the previous section. At 353 K, CO_2 solubility in each solvent is quite similar up to 2 MPa. Above this pressure the same trend than at 283 K is observed.

The detailed knowledge of the thermodynamic properties of the working fluid pairs is crucial to retrofit and modify absorption refrigeration process. In the field of refrigeration system, there is a strong need for experimental thermodynamic data, such as phase equilibria and energetic data. Furthermore, the process developments including the sizing of operation units, the estimation of process parameters and the simulation of the process plant, requires to dispose of an appropriate thermodynamic model. Therefore, to complete this study experimental measurements of calorimetric and transport properties will be performed on these promising {CO_2+BBS} systems. Excess enthalpies and enthalpies of solution ($\Delta_{sol}H$) will be determined using the flow calorimetric technique described in section 2.3.2. Specific heat capacities (Cp) and densities will also be determined for these systems. These experimental data will be then an imperious prerequisite to benchmark potentially usable thermodynamic models and fit model parameters.

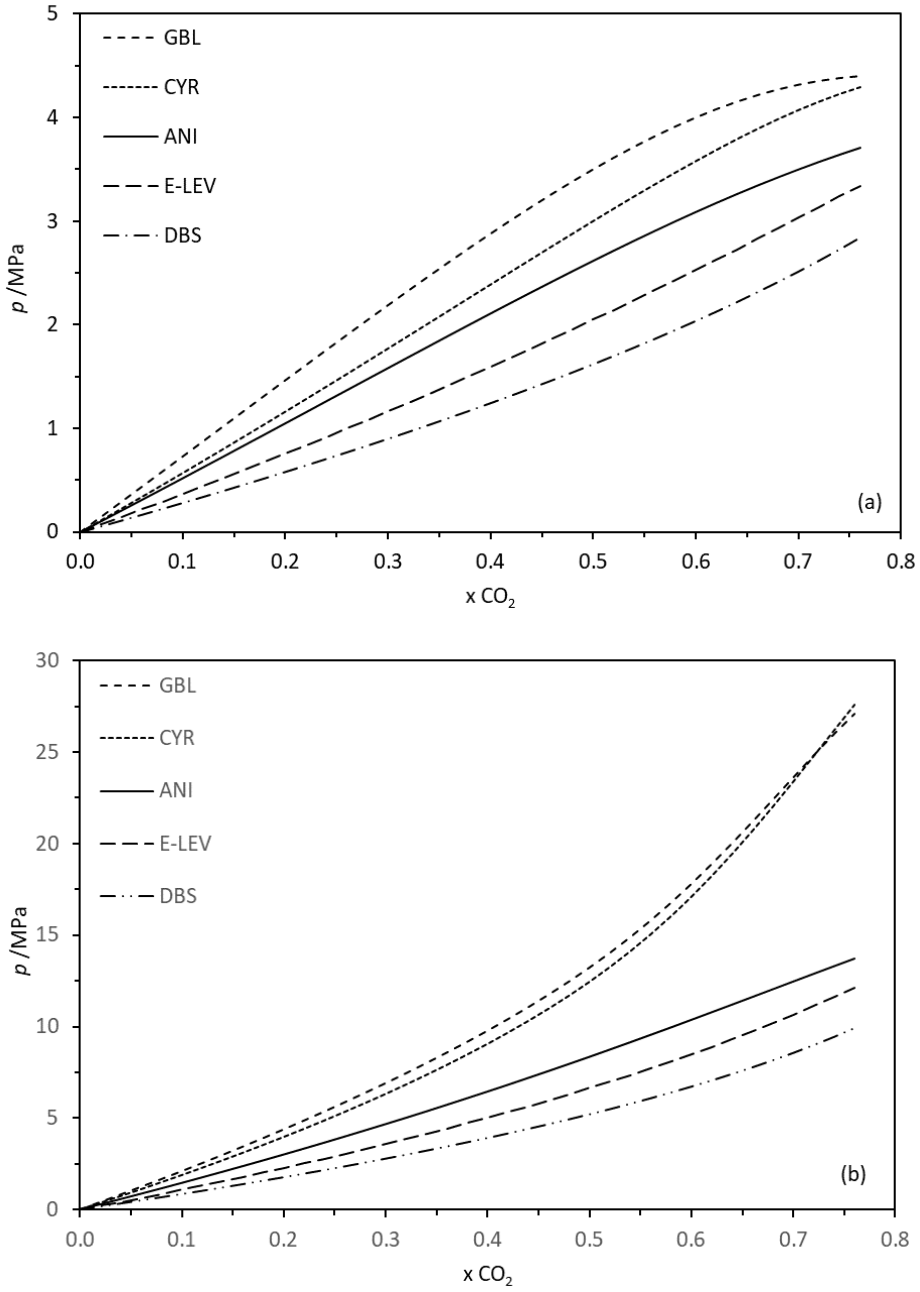

Figure 8. Comparison of five {CO_2-BBS} systems at (a) 283 K; (b) 353 K

4. CONCLUSIONS

In this paper a methodology aimed at selecting biobased solvents to be used in a vapor absorption refrigeration cycle was proposed. The first step of this approach was based on the use of molecular descriptors to identify appropriate absorbents for the process. Five of them are presented in this study namely ethyl levulinate, γ-butyrolactone, dibutyl succinate, cyrene and anisole. To pursue this selection, CO_2 solubility in these solvents was investigated. Indeed, the high solubility of the refrigerant in the absorbent being one of the most important criteria for the process, the knowledge of the vapor-liquid equilibrium of {CO_2+BBS} systems is required. Nevertheless, experimental VLE data are relatively scarce in the literature at the operating conditions of temperature and pressure of the process. New experimental VLE data were thus determined for {CO_2+cyrene} system using a flow calorimetric and a spectroscopic technique at 313.15 K and pressure from 0.5 to 4.00 MPa. To predict this thermodynamic property, molecular simulations were performed on these five bio-based solvents. Also a thermodynamic model capable of reproducing phase equilibria was developed. It allowed the selection of the most promising bio-based solvents namely ethyl levulinate, dibutyl succinate and anisole.

ACKNOWLEDGEMENTS

The authors acknowledge financial support from the French projects ANR-20-CE05-0004 AWARE and PAI, supported by the French government ant the Auvergne Rhone Alpes region.

NOMENCLATURE

p	pressure (MPa)	R	molar gas constant (8.314472 J×mol^{-1}×K^{-1})
T	temperature (K)	V	molar volume (m^3×mol^{-1})
$\Delta_{sol}H$	enthalpy of solution (kJ×mol^{-1})	α	CO_2 loading charge (mol CO_2/mol absorbent)
x_{CO2}	CO_2 molar fraction in liquid phase	z	molar fraction in liquid or vapor phase
u	standard deviation	ω	acentric factor
k_{ij}	binary interaction parameter		

REFERENCES

Arcis, H., Ballerat-Busserolles, K., Rodier, L., Coxam, J.-Y., 2011, J. Chem. Eng. Data, 56(8), 3351-3362.
Baird, Z.S., Uusi-Kyyny, P., Pokki, J.-P., Pedegert, E., Alopaeus, V., 2019, Int. J. Thermophys., 40(11), 102.
Brugère, E., Andanson, J.-M., Ballerat-Busserolles, K., 2020. The Use of IR Spectroscopy to Follow the Absorption of CO2 in Amine Media – Evaluation of the Speciation with Time. In Ying Wu, John J. Carroll, Mingqiang Hao, and Zhu, W., Gas Injection into Geological Formations and Related Topics, Scrivener Publishing, 41-53.
Deng, D., Han, G., Jiang, Y., Ai, N., 2015, J. Chem. Eng. Data, 60(1), 104-111.
Dodda, L.S., Cabeza de Vaca, I., Tirado-Rives, J., Jorgensen, W.L., 2017, Nucleic Acids Res., 45(W1), W331-W336.
Giacomin Junior, W.R., Capeletto, C.A., Voll, F.A.P., Corazza, M.L., 2019, J. Chem. Eng. Data, 64(5), 2011-2017.

Gui, X., Wang, W., Wang, C., Zhang, L., Yun, Z., Tang, Z., 2014, J. Chem. Eng. Data, 59(3), 844-849.
Gwinner, B., Roizard, D., Lapicque, F., Favre, E., Cadours, R., Boucot, P., Carrette, P.-L., 2006, Ind. Eng. Chem. Res., 45(14), 5044-5049.
Jorgensen, W.L. ,Tirado-Rives, J., 2005, Proc. Natl. Acad. Sci. U.S.A., 102(19), 6665-6670.
Kim, C.H., Clark, A.B., Vimalchand, P., Donohue, M.D., 1989, J. Chem. Eng. Data, 34(4), 391-395.
Kim, Y.J., Kim, S., Joshi, Y.K., Fedorov, A.G., Kohl, P.A., 2012, Energy, 44(1), 1005-1016.
Li, X., Jiang, Y., Han, G., Deng, D., 2016, J. Chem. Eng. Data, 61(3), 1254-1261.
Lorentzen, G., 1994, Int. J. Refrigeration, 17(5), 292-301.
Macriss, R.A., Gutraj, J.M., Zawacki, T.S., 1988. Absorption fluids data survey: Final report on worldwide data, Oak Ridge National Lab., TN (USA); Institute of Gas Technology, Chicago, IL (USA).
Martínez, L., Andrade, R., Birgin, E.G., Martínez, J.M., 2009, J. Comput. Chem., 30(13), 2157-2164.
Mota-Babiloni, A., Makhnatch, P., Khodabandeh, R., 2017, Int. J. Refrigeration, 82, 288-301.
Park, S.D., Kim, C.H., Choi, C.S., 1991, J. Chem. Eng. Data, 36(1), 80-84.
Pasquali, I., Andanson, J.-M., Kazarian, S.G., Bettini, R., 2008, J. Supercrit. Fluids, 45(3), 384-390.
Perez-Blanco, H., 1984, Int. J. Refrigeration, 7(2), 115-122.
Redlich, O. ,Kwong, J.N.S., 1949, Chem. Rev., 44(1), 233-244.
Soave, G., 1972, Chem. Eng. Sci., 27(6), 1197-1203.
Span, R. ,Wagner, W., 1996, J. Phys. Chem. Ref. Data, 25(6), 1509-1596.
Srikhirin, P., Aphornratana, S., Chungpaibulpatana, S., 2001, Renew. Sust. Energ. Rev., 5(4), 343-372.
Sun, J., Fu, L., Zhang, S., 2012, Renew. Sust. Energ. Rev., 16(4), 1899-1906.
Thompson, A.P., Aktulga, H.M., Berger, R., Bolintineanu, D.S., Brown, W.M., Crozier, P.S., in 't Veld, P.J., Kohlmeyer, A., Moore, S.G., Nguyen, T.D., Shan, R., Stevens, M.J., Tranchida, J., Trott, C., Plimpton, S.J., 2022, Comput. Phys. Commun., 271, 108171.
Wasserscheid, P. ,Seiler, M., 2011, ChemSusChem, 4(4), 459-463.
Xu, Q., Wagner, K.-D., Dahmen, N., 2003, J. Supercrit. Fluids, 26(2), 83-93.